

## Effect of sterol side-chain structure on sterol–phosphatidylcholine interactions in monolayers and small unilamellar vesicles

J. Peter Slotte <sup>a,\*</sup>, Marina Jungner <sup>a</sup>, Catherine Vilchère <sup>b</sup>, Robert Bittman <sup>b</sup>

<sup>a</sup> Department of Biochemistry and Pharmacy, Åbo Akademi University, P.O. Box 66, 20521 Turku, Finland,

<sup>b</sup> Department of Chemistry and Biochemistry, Queens College of the City University of New York, Flushing, NY, USA

(Received 8 July 1993)

### Abstract

In this study we have characterized the monolayer behavior of analogues of cholesterol having different side-chain structures and their interaction with phosphatidylcholines in mixed monolayers and small unilamellar vesicles (SUVs). Two series of side-chain analogues of cholesterol were synthesized, one with an unbranched side chain (the n-series, from 3 to 7 carbons in length), and the other with a single methyl-branched side chain (the iso-series, from 5 to 10 carbons in length). The length and conformation of the sterol side chain markedly influenced both the mean molecular area of the pure sterols and their monolayer stability (i.e., collapse pressure). Shorter side chains gave smaller mean molecular areas and decreased monolayer stability. The sterols from the n-series also had smaller mean molecular areas than the corresponding sterols in the iso-series. In mixed 1,2-dipalmitoyl-*sn*-glycero-3-phosphocholine (DPPC)/sterol monolayers (equimolar ratio; at 22°C), all of the sterols tested decreased the monolayer stability as judged by the lower collapse pressure with sterol than without sterol. A similar trend was observed in mixed monolayers containing 1-stearoyl-2-oleoyl-*sn*-glycero-3-phosphocholine (SOPC), except that sterols from the iso-series with a chain length of 8 or 10 carbon atoms actually stabilized the monolayer compared with the sterol-free SOPC monolayer. The ability of the sterols to condense the molecular packing of DPPC was similar with all sterols (3–5% condensation at 10 mN/m), irrespective of the length or structure of the side chain. 5-Androsten-3 $\beta$ -ol, however, which lacks the side chain, did not at all condense the monolayer packing of DPPC. With SOPC mixed monolayers, all side chain containing sterols caused a 18–20% condensation (at 10 mN/m) of monolayer packing. The condensing effect of 5-androsten-3 $\beta$ -ol on SOPC packing was again much smaller (about 10%) compared with that of the side-chain sterols. The rate of sterol oxidation by cholesterol oxidase (at 37°C) in DPPC-containing SUVs increased as a function of increasing the side-chain length (iso-series). With sterols from the n-series, the same trend was seen, except that the n-C7 analogue was oxidized much slower than the n-C4, n-C5, and n-C6 analogues. With SOPC SUVs, a similar side-chain dependent oxidation pattern was observed. Our results support and extend previous knowledge about the importance of the sterol side chain in determining sterol–sterol and sterol–phospholipid interactions, both in mono- and bilayers.

**Key words:** Sterol; Phospholipid; Lipid–lipid interaction; Cholesterol oxidase; Monolayer membrane; SUV

### 1. Introduction

Cholesterol is an ubiquitous structural and functional component of most eukaryotic plasma membranes. The structure of cholesterol has most likely evolved in order to allow for an optimal interaction of the sterol with various phospholipids and proteins in

the membranes [1,2]. The tetracyclic ring structure gives the cholesterol molecule its necessary rigidity, whereas the 3 $\beta$ -hydroxy group provides an important amphiphilic function [2]. In addition, cholesterol has an eight-carbon branched side chain, which may give the molecule unique properties. It is well known that cholesterol, bearing the iso-octyl side chain at C-17, can reduce the solute permeability of phosphatidylcholine (PC) liposomes, whereas a sterol analogue lacking a side chain (5-androsten-3 $\beta$ -ol) cannot [3]. The effect of cholesterol on the order parameter in phospholipid bilayers is also very dependent on the iso-octyl side

\* Corresponding author. Fax: +358 21 654745.

Abbreviations: PC, phosphatidylcholine; SUV, small unilamellar vesicles; DPPC, dipalmitoyl-PC; SOPC, 1-stearoyl-2-oleoyl-PC.

chain, since both shorter and longer side-chain-containing sterols are less effective as rigidifiers than cholesterol [4–6]. The side-chain structure of a sterol has further been shown to markedly affect the rate of intestinal absorption [7–9]. Although the mechanistic explanation for the effects of the side-chain structure on rates of sterol absorption is still unresolved, Kan and Bittman [10] have shown that the rate of sitosterol desorption from PC bilayers is markedly lower than that of cholesterol. Furthermore, the side-chain structure of the sterol affects the rate of transbilayer movement across the membrane bilayer of growing mycoplasma cells [11]. The rates of interactions of sterols with the polyene antibiotics amphotericin B and filipin in SUVs were also dependent on sterol side-chain structure [12].

However, the effect of cholesterol on the main transition enthalpy of a series of PCs was reported to not depend on the presence of a side chain, since 5-androsten-3 $\beta$ -ol was equally effective as cholesterol in removing the main phase transition of PC in bilayers over a similar range of sterol content [13,14]. However, infrared studies indicated that the acyl chains of DPPC are more disordered in bilayers containing 5-androsten-3 $\beta$ -ol than in those containing cholesterol [15]. Although monolayer studies have shown that a sterol needs a side chain in order to condense the lateral packing of PC, the length of the side chain appears to be less critical [5]. The aim of this study was to compare the monolayer stability of various sterol analogues with side chains of differing length and structure, both in pure and mixed PC-containing monolayers. This study also utilized the enzyme cholesterol oxidase as a probe for sterol oxidizability in SUVs prepared either from saturated (DPPC) or mono-unsaturated (SOPC) phospholipids.

## 2. Experimental procedures

**Materials.** Cholesterol, DPPC, and SOPC were obtained from Sigma. Each compound gave a single spot on thin-layer chromatography, and cholesterol was judged to be 99% pure by gas chromatography (see below). Cholesterol oxidase (*Streptomyces* sp.) was obtained from Calbiochem. The water used was purified by reverse osmosis, followed by passage through a MilliQ UF plus purification unit, to give a resistivity of less than 15 M $\Omega$ /cm.

**Synthesis of sterols with various side chains.** All of the sterols (see Fig. 1 for the structures of sterols used), except the iso-C5 compound, were synthesized using the method described by Morisaki et al. [16]. In this method, 22-tosyloxybisanorchole-5-en-3 $\beta$ -ol tetrahydropyranyl ether (**1**) was used as the key intermediate. The latter was prepared from bisnorcholeonic acid by

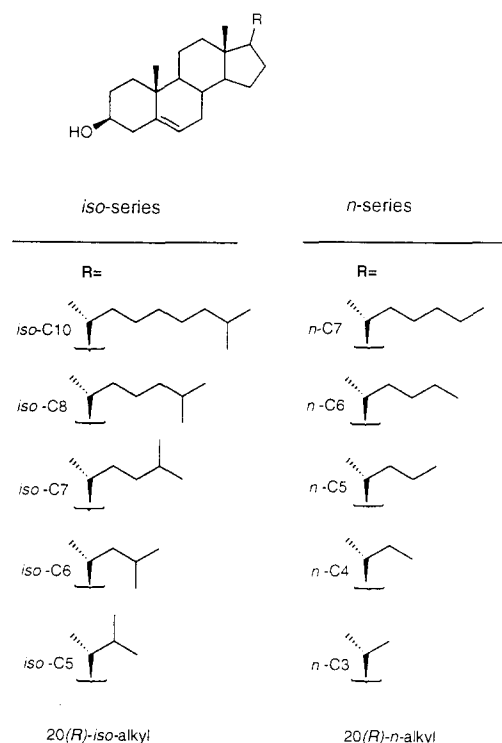


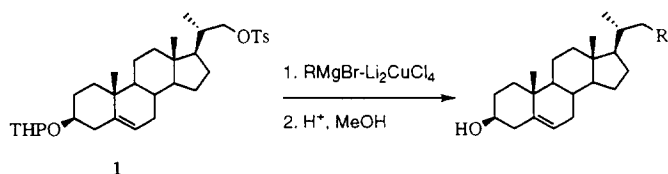
Fig. 1. Structures of the sterols used. The following abbreviations are used for the synthetic sterols: n-C3, 20(*R*)-methyl-5-pregnen-3 $\beta$ -ol; n-C4, 20(*R*)-ethyl-5-pregnen-3 $\beta$ -ol; n-C5, 20(*R*)-n-propyl-5-pregnen-3 $\beta$ -ol; n-C6, 20(*R*)-n-butyl-5-pregnen-3 $\beta$ -ol; n-C7, 20(*R*)-n-pentyl-5-pregnen-3 $\beta$ -ol; iso-C5, 20(*R*)-isopropyl-5-pregnen-3 $\beta$ -ol; iso-C6, 20(*R*)-isobutyl-5-pregnen-3 $\beta$ -ol; iso-C7, 20(*R*)-isopentyl-5-pregnen-3 $\beta$ -ol; iso-C8, 20(*R*)-isooctyl-5-pregnen-3 $\beta$ -ol (cholesterol); iso-C10, 20(*R*)-isoheptyl-5-pregnen-3 $\beta$ -ol. The number in the code name (e.g., iso-C10) refers to the total number of carbon atoms in the group attached to C-17 of the sterol.

THP etherification of the C-3 hydroxyl group, reduction of the carboxylic acid group with lithium aluminum hydride in THF and tosylation of the resulting primary alcohol. From the 22-tosylate **1**, the sterols (except the n-C3 and iso-C5 compounds) were obtained by copper-catalyzed coupling reaction with different alkylmagnesium bromides in the presence of Li<sub>2</sub>CuCl<sub>4</sub>, followed by acid-catalyzed hydrolysis of the THP ether (Scheme 1).

The n-C3 compound was obtained in 96% yield by hydrogenolysis of the 22-tosylate using lithium aluminum hydride (Scheme 2).

The iso-C5 compound was prepared directly from bisnorcholeonic acid by action of methylolithium to obtain the methyl ketone, Wittig reaction to yield the 22-methylene derivative, and specific reduction of the side-chain double bond by catalytic hydrogenation (Scheme 3).

The sterols were purified by flash chromatography and recrystallization from methanol. All of the compounds were fully characterized by <sup>1</sup>H-NMR spectroscopy.

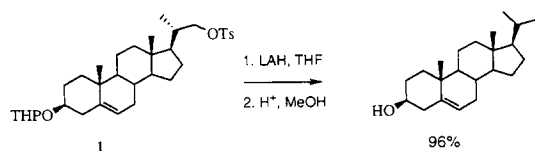


| RMgBr                                 | COMPOUND | CODE NAME | YIELD (%) <sup>a</sup> |
|---------------------------------------|----------|-----------|------------------------|
| MeMgBr                                |          | n-C4      | 81                     |
| EtMgBr                                |          | n-C5      | 75                     |
| n-PrMgBr                              |          | n-C6      | 62                     |
| i-PrMgBr                              |          | iso-C6    | 56                     |
| n-BuMgBr                              |          | n-C7      | 80                     |
| i-BuMgBr                              |          | iso-C7    | 71                     |
| i-C <sub>7</sub> H <sub>15</sub> MgBr |          | iso-C10   | 52                     |

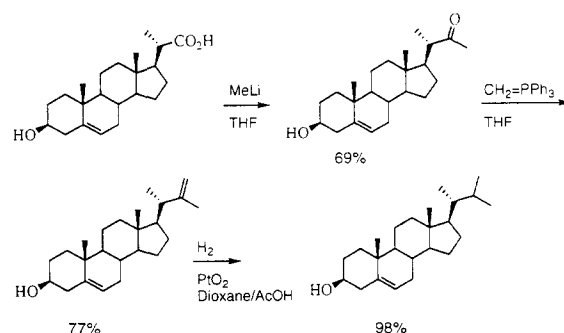
Scheme 1. Synthesis of sterols via copper-catalyzed Grignard coupling reaction. <sup>a</sup> Yields were reported based on bisnorcholelenic acid as the starting material.

**General procedures.** THF was distilled over lithium aluminum hydride and stored over type 3Å molecular sieves. Silica gel TLC plates of a 0.25-mm thickness from Analtech, Newark, DE, were used to monitor reactions, and compounds were detected by spraying with 10% sulfuric acid in ethanol. E. Merck silica gel 60 (230–400 ASTM mesh) was used for flash chromatography. <sup>1</sup>H-NMR spectra were recorded on a 200-MHz Bruker spectrometer.

**Assessment of purity.** The purity of the synthetic sterols was assessed by gas-liquid chromatography on a Rtx-1 capillary column (100% dimethyl polysiloxane; Restec, PA, USA). The sterols were silylated before analysis [17]. The temperature program used was from 260°C to 280°C at 5°C/min, the injector temperature



Scheme 2. Synthesis of the nn-C3 sterol by hydride displacement of the 22-tosylate 1.



Scheme 3. Synthesis of the iso-C5 sterol via the 22-keto intermediate.

was 260°C, and the FID detector was maintained at 300°C. All of the synthetic sterols were found to be more than 98% pure.

**Quantitation of sterol stock solutions.** Stock solutions of sterols in hexane/2-propanol were matched against a calibrated cholesterol stock solution by a cholesterol oxidase assay, essentially as described by Heider and Boyett [18].

**Force–area isotherms in pure and mixed monolayers.** Force–area isotherms were determined for pure and mixed sterol/phospholipid (DPPC or SOPC) monolayers using a KSV 3000 Surface Barostat (KSV Instruments, Helsinki). The isotherms were run in a rectangular teflon trough (450 mm × 60 mm) on water at 22°C. Stock solution of the lipids were prepared in hexane/2-propanol (3:2 v/v), and were stored at –20°C. The lipid solution was spread on the aqueous surface, and the monolayer was allowed to stabilize for 5 min before it was compressed at a barrier speed not exceeding 6 Å<sup>2</sup>/molecule per min. Data were sampled every 2 s. At least two different runs were performed at each lipid composition, and the reproducibility was better than ±2%. The extent of phospholipid condensation by the sterols in mixed monolayers was assessed and calculated as described previously [19].

**Preparation of SUVs.** Small unilamellar vesicles were prepared from different sterols and either DPPC or SOPC, dissolved in absolute ethanol, by injection into the reaction buffer (Dulbecco's phosphate-buffered saline, containing 5 U/ml of horseradish peroxidase, and 0.15 mg/ml of *p*-hydroxyphenylacetic acid). The sterol/phospholipid molar ratio was 1.25:1. The ethanol injection was performed with a spring-loaded Hamilton syringe (the speed of the ejection was in the order of 0.1 s), and the final ethanol concentration was less than 1 vol% in the final SUV preparation. The resulting SUV suspension was optically clear, and was used 60–90 min after preparation (this time period was used to equilibrate the SUV preparations at 37°C). A size distribution characterization (using a Malvern laser light scattering equipment [20]) of ethanol-injected SUV:s indicated that the average diameter was smaller than 40 nm in diameter (data not shown).

**Oxidation of sterol by cholesterol oxidase in SUVs.** The SUVs containing different sterols and either DPPC or SOPC were prepared in a complete reaction buffer (Dulbecco's phosphate-buffered saline, 0.15 mg/ml of *p*-hydroxyphenyl acetic acid, 5 U/ml of horseradish peroxidase) minus cholesterol oxidase. A 1.5-ml aliquot (which was kept at 37°C protected from ambient light) was transferred to a quartz cuvette, which was in turn placed in a Hitachi F2000 spectrofluorometer thermostatted to 37°C. The excitation wavelength was 325 nm, and the emission was read at 415 nm. To initiate the oxidation, cholesterol oxidase was added to a final concentration of 133 mU/ml. The oxidation reaction was followed during a 10-min recording, with continuous mixing (200 rpm) in the cuvette. The interpretation of the resulting oxidation curve is given in Fig. 5.

### 3. Results

#### Monolayers of pure sterols

Force–area isotherms of pure sterol analogues were obtained on water at 22°C. A typical sterol isotherm (e.g., cholesterol) is shown in Fig. 2, and the values (i.e., the mean molecular area at zero surface pressure,  $A_0$ ; the maximal surface pressure before collapse of the monolayer,  $\pi_{c1}$ ; and the equilibrium collapse pressure observed upon continuous collapse of the monolayer,  $\pi_{c2}$ ) derived from the various isotherms are defined in this Figure. The  $A_0$  values for each sterol are given in Table 1. It can generally be noted that the  $A_0$  value is smaller for sterols with shorter side chains compared with those having longer side chains. It also appeared that the branched side-chain analogues (iso-series) were larger than the unbranched side-chain

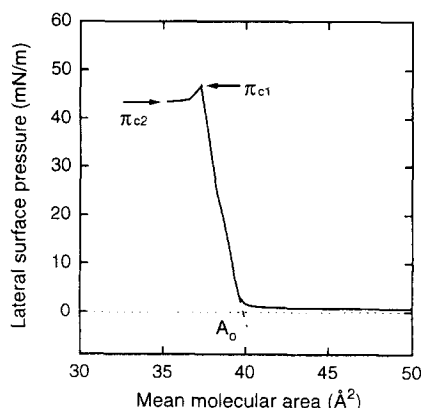


Fig. 2. Force–area isotherm of cholesterol. Similar force–area isotherms were obtained for all of the sterols, and the extracted data are presented in Table 1.  $A_0$  is the extrapolated mean molecular area at zero surface pressure.  $\pi_{c1}$  is the maximal obtainable surface pressure, at which the monolayer starts to collapse, whereas  $\pi_{c2}$  is the equilibrium collapse pressure, upon continued compression of the monolayer.

Table 1

Monolayer characteristics of sterols containing various side chains

| Side chain length | $A_0$ ( $\text{\AA}^2$ ) <sup>a</sup> | $\pi_{c1}$ (mN/m) <sup>b</sup> | $\pi_{c2}$ (mN/m) <sup>c</sup> | $\Delta$ <sup>d</sup> |
|-------------------|---------------------------------------|--------------------------------|--------------------------------|-----------------------|
| iso-C10           | 40.7                                  | 47                             | 38                             | 9                     |
| iso-C8            | 40.2                                  | 49                             | 44                             | 5                     |
| (cholesterol)     |                                       |                                |                                |                       |
| iso-C7            | 40.8                                  | 47                             | 39                             | 8                     |
| n-C7              | 39.9                                  | 43                             | 34                             | 9                     |
| iso-C6            | 41.7                                  | 48                             | 35                             | 13                    |
| n-C6              | 40.2                                  | 44                             | 34                             | 10                    |
| iso-C5            | 41.6                                  | 41                             | 23                             | 18                    |
| n-C5              | 38.3                                  | 43                             | 31                             | 12                    |
| n-C4              | 38.3                                  | 41                             | 32                             | 9                     |
| n-C3              | 37.8                                  | 40                             | 36                             | 4                     |
| H                 | 38.7                                  | 35                             | 35                             | 0                     |

Force–area isotherms of pure sterols on water at 22°C were collected and analyzed as described in Fig. 2. Values are averages of three or four different isotherms for each sterol.

<sup>a</sup> The limiting mean molecular area at zero surface pressure.

<sup>b</sup> Maximal surface pressure before initiation of collapse.

<sup>c</sup> Equilibrium collapse pressure.

<sup>d</sup> Difference between  $\pi_{c1}$  and  $\pi_{c2}$ .

analogues (n-series): iso-C7 had a 2.25% larger mean molecular area than n-C7, iso-C6 was 3.7% larger than n-C6, and iso-C5 was 8.6% larger than n-C6.

All of the sterols displayed fairly condensed isotherms, similar to that shown for cholesterol (Fig. 2), with compressibility values below  $3 \cdot 10^{-3}$  m/mN (data not shown). The stability of the compressed monolayer was clearly dependent on the conformation and length of the sterol side chain (Fig. 3). The maximal surface pressure obtained before collapse of the monolayer ( $\pi_{c1}$ ) was highest with analogues having a branched side chain longer than or equal to 6 carbons (Fig. 3A). With unbranched side chains, the  $\pi_{c1}$  value decreased almost linearly from side chains of 6 carbons down to zero (5-androsten-3 $\beta$ -ol) (Fig. 3B). The difference between  $\pi_{c1}$  and  $\pi_{c2}$  ( $\pi_{c2}$  being the equilibrium collapse pressure) was also clearly dependent on the side chain (Fig. 3C,D), so that monolayers of a sterol with a 5-carbon side chain (both iso and n-series) displayed the largest difference between  $\pi_{c1}$  and  $\pi_{c2}$ . With the n analogues, the difference between  $\pi_{c1}$  and  $\pi_{c2}$  decreased with decreasing chain length, and was zero for 5-androsten-3 $\beta$ -ol. It should be observed that the collapse behavior of monolayers markedly depend on the compression rate applied (in our case about 6  $\text{\AA}^2/\text{molecule, min}$ ). However, since the different sterol monolayers were compressed identically, the observed differences in collapse pressures are likely to be due to the variation in the molecular structure of the sterols.

#### Monolayers of sterols and phospholipids

Force–area isotherms of mixed sterol/phospholipid monolayers were made in order to evaluate the condensing effect of the various sterols on the packing

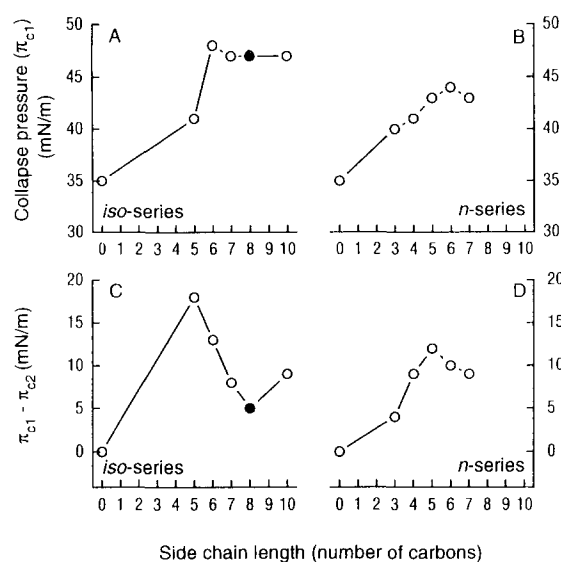


Fig. 3. Monolayer collapse properties of pure sterols at the water/air interface. The maximal obtainable lateral surface pressure ( $\pi_{c1}$  as defined in Fig. 2) is plotted against the side chain length (the iso-series in panel A, and the n-series in panel B). The difference between the maximal obtainable lateral surface pressure ( $\pi_{c1}$ ) and the equilibrium collapse pressure ( $\pi_{c2}$ ) is plotted against the side-chain length (panel C for the iso-series, and panel D for the n-series). The filled dot represents cholesterol ('iso-C8').

properties of the phospholipid. The results from such studies are presented in Table 2. With DPPC-containing mixed monolayers (at 50 mol% each of the sterol

Table 2  
Effects of sterol side-chain structure on DPPC packing in mixed monolayers

| Side chain length | $A_{10 \text{ mN/m}}$ ( $\text{\AA}^2$ ) <sup>a</sup> | $A_{\text{mix}, 10 \text{ mN/m}}$ ( $\text{\AA}^2$ ) <sup>b</sup> | % Condensation <sup>c</sup> |
|-------------------|---|---|-----------------------------|
| iso-C10           | 40.1  | 42.0  | 3.4                         |
| iso-C8            | 39.2  | 41.0  | 4.8                         |
| (cholesterol)     |   |   |                             |
| iso-C7            | 39.7  | 42.0  | 3.0                         |
| n-C7              | 39.0  | 41.0  | 4.5                         |
| iso-C6            | 41.2  | 42.2  | 4.2                         |
| n-C6              | 39.9  | 41.8  | 3.7                         |
| iso-C5            | 41.0  | 43.2  | 1.7                         |
| n-C5              | 37.9  | 40.2  | 5.2                         |
| n-C4              | 38.0  | 40.8  | 3.9                         |
| n-C3              | 37.4  | 40.2  | 4.6                         |
| H                 | 37.8  | 42.6  | 0                           |
| DPPC              | 46.9  |   |                             |

Force–area isotherms of pure sterols and DPPC, or mixed (1:1 molar ratio) sterol and DPPC monolayers were collected on water at 22°C. The mean molecular area at a surface pressure of 10 mN/m was determined for the pure and mixed monolayers, and the % condensation was calculated as described under Experimental procedures. Each value is the average of three or four isotherms.

<sup>a</sup> Mean molecular area of the pure compound at 10 mN/m.

<sup>b</sup> Mean molecular area of the equimolar sterol/DPPC mixed monolayer at 10 mN/m.

<sup>c</sup> Percent condensation relative to an ideal mixture.

Table 3  
Effects of sterol side-chain structure on SOPC packing in mixed monolayers

| Side chain length | $A_{10 \text{ mN/m}}$ ( $\text{\AA}^2$ ) <sup>a</sup> | $A_{\text{mix}, 10 \text{ mN/m}}$ ( $\text{\AA}^2$ ) <sup>b</sup> | % Condensation <sup>c</sup> |
|-------------------|---|---|-----------------------------|
| iso-C10           | 40.1  | 45.9  | 19.2                        |
| iso-C8            | 39.2  | 45.2  | 19.8                        |
| (cholesterol)     |   |   |                             |
| iso-C7            | 39.7  | 45.7  | 19.3                        |
| n-C7              | 39.0  | 45.7  | 18.8                        |
| iso-C6            | 41.2  | 46.9  | 18.2                        |
| n-C6              | 39.9  | 45.2  | 20.3                        |
| iso-C5            | 41.0  | 48.5  | 15.3                        |
| n-C5              | 37.9  | 45.0  | 19.2                        |
| n-C4              | 38.0  | 46.5  | 16.6                        |
| n-C3              | 37.4  | 45.5  | 18.0                        |
| H                 | 37.8  | 50.2  | 9.8                         |
| SOPC              | 73.5  |   |                             |

Force–area isotherms of pure sterols and SOPC, or mixed (1:1 molar ratio) sterol and SOPC monolayers were collected on water at 22°C. The mean molecular area at a surface pressure of 10 mN/m was determined for the pure and mixed monolayers, and the % condensation was calculated as described under Experimental procedures. Each value is the average of three or four isotherms.

<sup>a</sup> Mean molecular area of the pure compound at 10 mN/m.

<sup>b</sup> Mean molecular area of the equimolar sterol/SOPC mixed monolayer at 10 mN/m.

<sup>c</sup> Percent condensation relative to an ideal mixture.

and phospholipid), all side-chain-containing sterols displayed the well-known condensing effect (3–5% area reduction; values given at 10 mN/m). The magnitude of the effect was similar with all sterols, except for the iso-C5 derivative, which showed a smaller effect than the other sterols tested. 5-Androsten-3 $\beta$ -ol, which lacks a side chain, had no condensing effect on the packing of DPPC in monolayers.

Similar findings were observed with SOPC mixed monolayers (Table 3). The condensing effect of the sterols did not differ much (accounting to a 18–20% area reduction), except that iso-C5 and n-C4 appeared to have a smaller condensing effect than the others. Again, 5-androsten-3 $\beta$ -ol gave the smallest condensation of the packing density of SOPC.

The influence of the sterol side chain on monolayer stability was also examined in mixed monolayers containing equimolar amounts of one of the sterols and either DPPC or SOPC. The degree of monolayer stability was assessed from the collapse pressure of the monolayer. In mixed monolayers, only one collapse pressure was observed (corresponding to  $\pi_{c1}$ ), since the maximal obtainable lateral surface pressure at collapse was also the equilibrium collapse pressure (curve not shown). The variation of the collapse pressure versus side-chain length is given in Fig. 4. The collapse pressure of mixed monolayers containing sterols and DPPC was in all cases lower than the collapse pressure of the pure DPPC monolayer (dashed line in Fig. 4A,B).

Further, both with the iso and n-series, the collapse pressure decreased with decreasing side-chain length. The collapse pressure in equimolar mixed monolayers was always higher than the  $\pi_{cl}$  observed in pure sterol monolayers, indicating that the sterols were miscible in the phospholipid environment at this concentration.

In SOPC mixed monolayers, the collapse pressure was also a function of sterol side-chain length, so that the collapse pressure decreased with decreasing side-chain length (Fig. 4C, D). The monolayers containing iso-C8 (cholesterol) and iso-C10 had slightly but reproducibly higher collapse pressures than pure SOPC, indicating that these sterols appeared to stabilize the monolayer compared with the pure SOPC monolayer.

#### Oxidation of sterols in phospholipid SUVs

In order to determine the degree of sterol–phospholipid interaction in SUVs, cholesterol oxidase was used as a probe. The activity of this enzyme at the water/lipid interface is markedly affected by the degree of lipid packing density (and consequently surface pressure) of the substrate-containing membrane [19,21]. It has been postulated that the desorption of the substrate molecule from the membrane to the active site of the enzyme is the major rate-limiting step in the conversion of a  $3\beta$ - $\Delta^5$ -sterol to its 3-keto- $\Delta^4$  product [22]. Since this desorption step is thought to be influenced by packing density and molecular interactions (i.e., sterol–sterol or sterol–phospholipid), the cholesterol oxidase reaction appears to be a good tool to

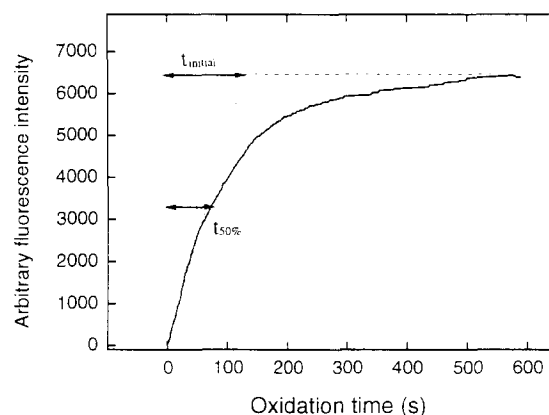


Fig. 5. Oxidation profile of a sterol in phospholipid (e.g., SOPC) vesicles. Vesicles of either DPPC or SOPC were prepared to contain 125 nmol sterol per 100 nmol phospholipid. A total of 125 nmol sterol per ml of buffer was oxidized at 37°C by 133 mU/ml cholesterol oxidase. The extracted data are presented in Table 4. The oxidation rate is given as the (a)  $t_{\text{initial}}$ , the time needed to obtain maximal oxidation as estimated from the tangent to the initial rate, and (b)  $t_{50\%}$ , the time needed to give 50% of the maximal oxidation obtained after a reaction period of 600 s.

probe for differences in sterol–lipid interactions in model membrane systems.

SUVs containing either DPPC or SOPC (100 nmol/ml) and one of the side-chain analogues (125 nmol/ml) were prepared by ethanol injection, and

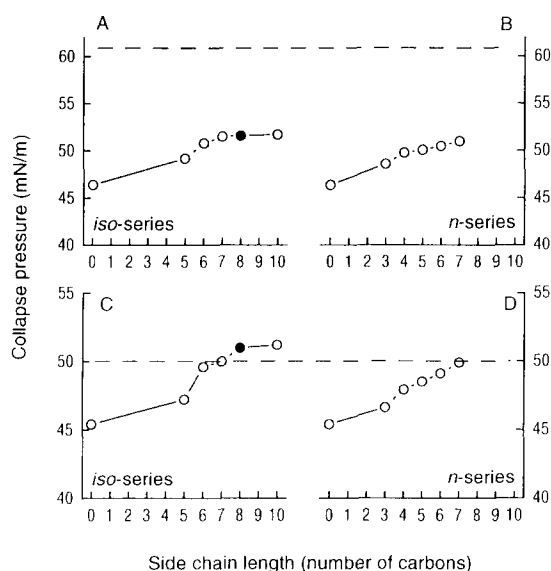


Fig. 4. Monolayer collapse pressures in mixed sterol/phospholipid monolayers. The collapse surface pressure for mixed monolayers of different sterols and either DPPC or SOPC (at 50 mol% sterol and phospholipid, respectively) were obtained, and values are plotted against the side-chain length (the iso-series in panels A and C, and the n-series in panels B and D, for DPPC (A and B) and SOPC (C and D), respectively).

Table 4  
Susceptibility of sterols containing various side chains to oxidation by cholesterol oxidase in SUVs prepared from either DPPC or SOPC

| Side chain structure | DPPC vesicles <sup>a</sup>            |                             | SOPC vesicles            |                |
|----------------------|---------------------------------------|-----------------------------|--------------------------|----------------|
|                      | $t_{\text{initial}}$ (s) <sup>b</sup> | $t_{50\%}$ (s) <sup>c</sup> | $t_{\text{initial}}$ (s) | $t_{50\%}$ (s) |
| iso-C10              | 29 ± 5                                | 73 ± 8                      | 36 ± 4                   | 16 ± 1         |
| iso-C8 (cholesterol) | 245 ± 35                              | 100 ± 5                     | 15 ± 5                   | 15 ± 2         |
| iso-C7               | 240 ± 30                              | 115 ± 5                     | 22 ± 3                   | 10 ± 1         |
| n-C7                 | 260 ± 10                              | 120 ± 10                    | 90 ± 10                  | 55 ± 3         |
| iso-C6               | 55 ± 5                                | 65 ± 5                      | 120 ± 5                  | 70 ± 5         |
| n-C6                 | 65 ± 5                                | 35 ± 5                      | 22 ± 3                   | 17 ± 2         |
| iso-C5               | 170 ± 25                              | 105 ± 10                    | 400 ± 50                 | 210 ± 30       |
| n-C5                 | 25 ± 1                                | 45 ± 5                      | 105 ± 5                  | 70 ± 5         |
| n-C4                 | 50 ± 1                                | 65 ± 5                      | 177 ± 3                  | 110 ± 10       |
| n-C3                 | 235 ± 20                              | 145 ± 15                    | 260 ± 10                 | 130 ± 5        |
| H                    | 285 ± 15                              | 185 ± 5                     | 350 ± 10                 | 210 ± 20       |

Small unilamellar vesicles of 125 nmol/ml sterol and 100 nmol/ml phospholipid (either DPPC or SOPC) were prepared by ethanol injection (see Experimental procedures) into phosphate-buffered saline. The oxidation of sterol in SUVs was performed as described under Experimental procedures. Each value is the average of three different experiments, with at least two different preparations of SUVs.

<sup>a</sup> Sterol/DPPC or sterol/SOPC vesicles with a sterol/phospholipid ratio of 1.25 to 1.0.

<sup>b</sup> Reaction time to give maximal oxidation with initial kinetics.

<sup>c</sup> Observed reaction time to give 50% of maximal oxidation (see Fig. 3 and caption for definitions).

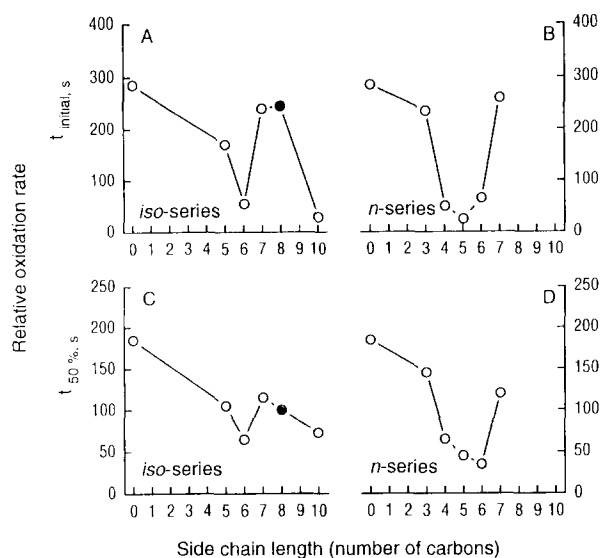


Fig. 6. Relative times needed for oxidation of sterols in DPPC SUVs by cholesterol oxidase. The upper panels give the  $t_{\text{initial}}$  versus sterol side-chain lengths, i.e., the time needed for maximal oxidation if initial kinetics were followed (panel A for the iso-series and panel B for the n-series), whereas the lower panels give the  $t_{50\%}$  values versus side-chain length, i.e., the time needed to give 50% oxidation (panel C for the iso-series and panel D for the n-series).

were equilibrated for 60–90 min before exposure of SUVs to cholesterol oxidase. The values collected from the oxidation studies are defined in Fig. 5. Based on each oxidation curve (collected during a 10-min reaction period), we calculated the time needed for maximal oxidation based on initial rates ( $t_{\text{initial}}$ ), and the

actual time needed for half-maximal oxidation ( $t_{50\%}$ ). Generally, the calculated  $t_{\text{initial}}$  and the actual  $t_{50\%}$  values showed similar trends with regard to the side-chain structure (Table 4). With SUVs prepared from DPPC, the oxidation time increased with decreasing side-chain length, except for the iso-C6 analogue, which was oxidized faster than either iso-C7 or iso-C5 (Fig. 6 A,C). With the analogues of the n-series, compounds with 4, 5, and 6 carbons in the side chain were oxidized markedly faster than the shorter (3 and zero carbons) or the longer (7 carbons) analogues (Fig. 6B,D). With SUVs prepared from SOPC, the oxidation susceptibility of the sterols followed a similar pattern as described for the DPPC SUVs. The oxidation time (both  $t_{\text{initial}}$  and  $t_{50\%}$ ) increased markedly with decreasing side-chain length, both with the iso- and the n-analogues (Fig. 7A,C and B,D).

#### 4. Discussion

In this study we have examined the role of the cholesterol side chain in sterol–sterol and sterol–phospholipid interactions in monolayers and SUVs. As a measure of molecular interaction, we determined the collapse pressure in pure sterol monolayers (in part a measure of sterol–sterol interaction) and mixed phospholipid-containing monolayers (sterol–phospholipid interaction), and the extent of sterol-induced condensation of PC packing (sterol–phospholipid interaction). As a measure of sterol–phospholipid interaction in vesicles, we utilized cholesterol oxidase to probe the accessibility of the sterol  $3\beta$ -hydroxy group to the lipid-water interface.

The collapse pressure ( $\pi_{\text{cl}}$ ) of pure sterol monolayers was clearly dependent on the length and structure of the sterol side chain, suggesting a role for the side chain in stabilizing sterol–lipid interactions. Although the sterol side chain is flexible compared with the rigid tetracyclic sterol nucleus [23], it is still likely that the side chains can interact with neighboring aliphatic groups. Such van der Waals interactions between aliphatic segments become more pronounced the longer the interacting segments grow [24,25]. This readily explains the clear side-chain-length dependency of the collapse pressure ( $\pi_{\text{cl}}$ ). It was further observed that a iso-branched side chain gave stronger interlipid interactions compared with the corresponding straight-chain sterol analogue. The observation that branched side-chain analogues are more stable in monolayers than the non-branched analogues suggests how a sterol with a branched side chain (cholesterol) has evolved to become the ubiquitous sterol in most eukaryotic cell membranes [1].

Further characterization of the collapse phenomenon in pure sterol monolayers revealed a side-

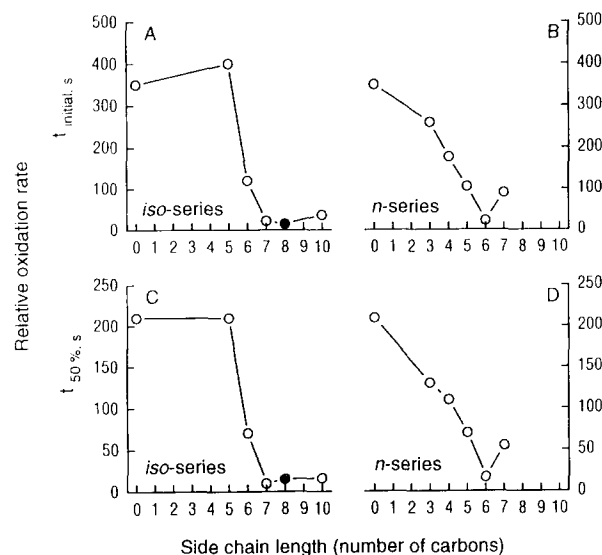


Fig. 7. Relative times needed for oxidation of sterols in SOPC SUVs by cholesterol oxidase. The upper panels give the  $t_{\text{initial}}$  versus sterol side-chain lengths (panel A for the iso-series and panel B for the n-series), whereas the lower panels give the  $t_{50\%}$  values versus side-chain length (panel C for the iso-series and panel D for the n-series).

chain dependent effect on the difference between the maximal obtainable pressure at collapse ( $\pi_{c1}$ ), and the 'equilibrium' collapse pressure ( $\pi_{c2}$ ) observed upon continuous compression of the pure sterol monolayer during collapse. Both with the iso and the n-series, it was found that the C5 side-chain analogue displayed the greatest difference between  $\pi_{c1}$  and  $\pi_{c2}$ . The collapse of a sterol monolayer (particularly that of cholesterol) is characterized by a first stage of monolayer separation and nucleation of a three-dimensional phase, and a second stage of growth of the nuclei formed in the first stage [26]. Although we do not have an explanation for the anomalous collapse behavior of the C5 analogues (iso and n-series) in pure sterol monolayers, it is possible that this particular side chain minimized the activation energy needed for the second phase, the growth of collapse nuclei.

The characterization of mixed sterol/phospholipid monolayers revealed clearly that all sterols, independent of the side-chain structure, were miscible in DPPC and SOPC mixed monolayers (1:1 molar ratio) at 22°C. This miscibility was evident both from the collapse behavior of the mixed monolayers and from the condensation effect of the sterols on the packing of the phospholipid molecules. First, the collapse pressure in equimolar sterol/phospholipid monolayers was always higher than the corresponding  $\pi_{c1}$  observed in a pure sterol monolayer, indicating the presence of intermolecular forces in the monolayer [27]. In addition, the collapse pressure of mixed monolayers was clearly a function of the sterol side-chain structure, as was observed for the pure sterol monolayers. This again suggests that longer side chains allow stronger intermolecular van der Waals forces to take place. The observation that the collapse pressure of mixed sterol/DPPC monolayers was markedly lower than the collapse pressure observed for a pure DPPC monolayer is in good agreement with the known randomizing effect that sterols have on phospholipids [2,28], since attractive van der Waals forces are expected to diminish when a gel state lipid (i.e., DPPC) is transformed to a liquid-crystal state (i.e., cholesterol/DPPC). With SOPC mixed monolayers, sterols in the iso-series with side-chain lengths of 8 and 10 carbon atoms actually stabilized the membrane, probably because these sterols induced an ordering effect on the liquid-crystal (fluid) SOPC phase [2].

Secondly, the miscibility of sterols with various side-chain structures in both DPPC and SOPC monolayers (1:1 molar ratio) was evident from the condensing effect displayed by these sterols. The condensation of molecular packing (i.e., the deviation of the observed mean molecular area from that expected based on pure molecular area additivity [27,29–31] always indicate a real complete or partial mixing behavior, and consequently the existence of intermolecular forces

in the monolayer [27]. However, the extent of sterol-induced condensation of DPPC mixed monolayers was significantly lower compared with the fluid SOPC mixed monolayer. The condensing effect of the different sterol analogues was not related to their side-chain length or structure, except for 5-androsten-3 $\beta$ -ol and possibly the C5 analogues (both iso and n-series). 5-Androsten-3 $\beta$ -ol, which lacks a side chain, did not condense the packing of DPPC, and its condensing effect on SOPC monolayers was only half of that observed with side-chain containing sterols. Similar and concordant results on the effect of the sterol side chain on the monolayer condensation of phospholipids were reported previously [5]. These previous reports, together with our data, clearly establish the importance of the sterol side chain in sterol/phospholipid association.

The rate of oxidation of membrane-associated cholesterol by cholesterol oxidase is known to be sensitive to the degree of lateral packing density of the membrane [19,21]. The lateral packing density is, on the other hand, mainly a function of existing intermolecular forces (mostly van der Waals forces). Therefore, differences in rates of cholesterol oxidase-catalyzed sterol oxidation can be used to predict the relative strength of molecular interactions in sterol/phospholipid membranes [19,32].

When sterol-enriched SUVs (125 nmol sterol per 100 nmol phospholipid) were exposed to cholesterol oxidase at 37°C, it was generally found that within the iso-series, sterols were oxidized faster when the side-chain length increased. With sterols from the n-series, the oxidation susceptibility was highest with intermediate side-chain lengths (4–6 carbons), whereas shorter or longer side-chain sterols were oxidized at a markedly slower rate. This observation was also seen with SUVs of both DPPC and SOPC, indicating that the differences in oxidation rates shown in Figs. 6A,C versus 6B,D and 7A,C versus 7B,D reflect differences in sterol-phospholipid interactions in the vesicle membranes. In monolayers, however, the rates of cholesterol oxidase-catalyzed oxidation of cholesterol and 5-androsten-3 $\beta$ -ol are not significantly different [33]; also, we have observed that iso-C10 is oxidized with similar kinetics as cholesterol, when presented to the enzyme as a pure sterol monolayer (Slotte, Jungner, Vilchèze and Bittman, unpublished observation).

In planar monolayers, the oxidation rate is mainly dependent on both the sterol-to-colipid stoichiometry (especially if sterol-rich clusters are present) and on the lateral packing density [34]. However, the influence of curvature of SUVs (with radii in the range of 12–20 nm) on the oxidation rates of sterols with various side-chain structures needs to be considered. A sterol with a short side chain has a smaller molecular volume than does a longer chain analogue. The van der Waals volumes of the different sterols were calculated using



computer modeling as described in ref. [35]. We estimated the molecular volumes of cholesterol and 5-androsten-3 $\beta$ -ol to be 410.1 Å<sup>3</sup> and 278.5 Å<sup>3</sup>, respectively. For each methylene group removed from the iso-octyl side chain, a 4% reduction in molecular volume occurs. In a highly curved membrane, it is therefore possible that short-chain sterols (with reduced volumes) pack differently as compared to sterols having larger volumes, thus leading to changed interfacial packing density and cholesterol oxidase susceptibility.

Taken together, the results of this work have clearly highlighted the importance of the sterol side chain on sterol–sterol and sterol–phospholipid interactions in model membrane systems.

## 5. Acknowledgements

This work was supported in part by grants from the Sigrid Juselius Foundation, the Borg Foundation, and the Academy of Finland (to J.P.S.), and in part by NIH Grant HL 16660 (to R.B.).

## 6. References

- [1] Bloch, K. (1976) in *Reflections in Biochemistry* (Kornberg, A., Korcker, B.L.H., Cornudella, Z. and Oro, J., eds.), Pergamon Press, Oxford.
- [2] Yeagle, P.L. (1985) *Biochim. Biophys. Acta* 822, 267–287.
- [3] Nakamura, T., Nishikawa, M., Inoue, K., Nojima, S., Akiyama, T. and Sankawa, U. (1980) *Chem. Phys. Lipids* 26, 101–110.
- [4] Suckling, K.E. and Boyd, G.S. (1976) *Biochim. Biophys. Acta* 426, 295–300.
- [5] Suckling, K.E., Blair, H.A.F., Boyd, G.S., Craig, I.F. and Malcolm, B.R. (1979) *Biochim. Biophys. Acta* 551, 10–21.
- [6] Craig, I.F., Boyd, G.S. and Suckling, K.E. (1978) *Biochim. Biophys. Acta* 508, 418–421.
- [7] Salen, G., Ahrens, E.H., Jr. and Grundy, S.M. (1970) *J. Clin. Invest.* 49, 952–967.
- [8] Bhattacharyya, A.K. (1981) *Am. J. Physiol.* 240, G50–55.
- [9] Ikeda, I., Tanaka, K., Sugano, M., Vahouny, G.V. and Gallo, L.L. (1988) *J. Lipid Res.* 29, 1583–1591.
- [10] Kan, C.-C. and Bittman, R. (1991) *J. Am. Chem. Soc.* 113, 6650–6656.
- [11] Clejan, S. and Bittman, R. (1984) *J. Biol. Chem.* 259, 449–455.
- [12] Clejan, S. and Bittman, R. (1985) *J. Biol. Chem.* 260, 2884–2889.
- [13] Singer, M.A. and Finegold, L. (1990) *Chem. Phys. Lipids* 56, 217–222.
- [14] Finegold, L. and Singer, M.A. (1993) in *Cholesterol in Membrane Models* (Finegold, L., ed.), pp. 137–157, CRC Press, Boca Raton, FL.
- [15] Senak, L., Moore, D., and Mendelsohn, R. (1992) *J. Phys. Chem.* 96, 2749–2754.
- [16] Morisaki, M., Shibata, M., Duque, C., Imamura, N. and Ikekawa, N. (1980) *Chem. Pharm. Bull.* 28, 606–611.
- [17] Slotte, J.P., Hedström, G., Rannström, S., and Ekman, S. (1989) *Biochim. Biophys. Acta* 985, 90–96.
- [18] Heider, J.G. and Boyett, R.L. (1978) *J. Lipid Res.* 19, 514–518.
- [19] Grönberg, L. and Slotte, J.P. (1990) *Biochemistry* 29, 3173–3178.
- [20] Hedström, G., Slotte, J.P., Molander, O. and Rosenholm, J.B. (1992) *Biotech. Bioeng.* 39, 218–224.
- [21] Slotte, J.P. (1992) *Biochim. Biophys. Acta* 1123, 326–333.
- [22] Slotte, J.P. and Östman, A.-L. (1993) *Biochim. Biophys. Acta* 1145, 243–249.
- [23] Duax, W.L., Griffin, J.F. and Rohrer, D.C. (1980) *Lipids* 15, 783–792.
- [24] Salem, L. (1962) *J. Chem. Phys.* 37, 2100–2113.
- [25] Lund-Katz, S., Laboda, H.M., McLean, L.R. and Phillips, M.C. (1988) *Biochemistry* 27, 3416–3423.
- [26] Baglioni, P., Cestelli, G., Dei, L. and Gabrielli, G. (1985) *J. Colloid Interf. Sci.* 104, 143–150.
- [27] Dörfler, H.-D. (1990) *Adv. Colloid Interf. Sci.* 31, 1–110.
- [28] Oldfield, E. and Chapman, D. (1972) *FEBS Lett.* 21, 303–306.
- [29] Leathes, J.B. (1925) *Lancet* 208, 853.
- [30] De Bernard, L. (1958) *Bull. Soc. Chim. Biol.* 40, 161.
- [31] Chapman, D., Owens, N.F., Phillips, M.C. and Walker, D.A. (1969) *Biochim. Biophys. Acta* 183, 458–65.
- [32] Grönberg, L., Ruan, Z.-s., Bittman, R. and Slotte, J.P. (1991) *Biochemistry* 30, 10746–10754.
- [33] Slotte, J.P. (1992) *Biochim. Biophys. Acta* 1124, 23–28.
- [34] Slotte, J.P. (1992) *Biochemistry* 31, 5472–5477.
- [35] Slotte, J.P. (1992) *J. Steroid. Biochem. Mol. Biol.* 42, 521–526.